Superstrings and the proton structure

Martin Schvellinger

Instituto de Física La Plata-CONICET &
Departamento de Física-UNLP

La Plata, Buenos Aires, Argentina

Seminar at the Jefferson Lab

March 25, 2024

A brief historical review

- 1960's: Hadron bootstrap models based on the S-matrix theory were developed, describing the hadron spectrum and hadron interactions.
- 1968: Veneziano's open string scattering amplitude for 2 to 2 mesons in Minkowski 4 dimensional spacetime:

  It leads to a soft behavior at high energy $s >> |t|$

  $$\text{cross section} \sim s^{\alpha(t)}$$

  with the linear Regge trajectory: $\alpha(t) = \alpha_1 t + \alpha_0$

A brief historical review

- 1968: first experiment of e+P DIS at SLAC led to:
  the discovery of the Bjorken scaling & the Feynman's parton model.
- 1973: QCD Lagrangian by Fritz, Gell-Mann & Leutwyller.
- 1974: Gross, Politzer & Wilzcek: asymptotic freedom.

A brief historical review

- 1974: Scherk & Schwarz: The Virasoro-Shapiro model, interpreted the massless spin-2 state of the model as a graviton, and also changed the Regge slope from 1 GeV^{-2} to the (Planck Mass)$^{-2}$.

  Birth of string theory as the theory of Quantum Gravity!!

- Thus, QCD and string theory describe very different physics!!!
- 1997: Maldacena: AdS/CFT correspondence which relates strongly coupled non-Abelian gauge theories to pertubative superstring theory.
- 2001: Polchinski & Strassler: hard scattering & DIS from string theory in terms of the AdS/CFT correspondence, obtaning the hard scattering behavior expected in QCD!! The crucial aspect is the propagation of strings in curved spacetime!! We will see that later in this talk.
- 2006: Brower, Polchinski, Strassler, Tan: BPST Pomeron (for F_2 Brower,Djuric, Minic, Tan)
- 2018: Kovensky, Michalski, Schvellinger: Holographic-A Pomeron for the proton helicity function g_1

Proton structure

- 1968: SLAC e+P DIS experiments.
- 1970's: DGLAP evolution equations from pQCD.
- 1977: The BFKL Pomeron.
- 1992-2007: HERA experiment testing F_2 with very high precisition.
- Testing QCD at LO, NLO, and currently at NNLO and beyond.
- On the other hand, since DGLAP approach is based on pQCD, at some point it becomes inadequate.
- Next generation Electron Ion Collider will extend the precision measurement to polarized proton structure, which requires to explore alternatives to DGLAP...

  This is where the present work begins.

The general idea of this work

- Explore the BPST Pomeron for F_2 and compare its predictions with experimental data and DGLAP predictions at LO, NLO and NNLO pQCD.
- Confront the new Holographic A Pomeron with the antisymmetric structure function g_1
- Give sharp predictions for g_1 in the range where the Electron Ion Collider will measure g_1 with very high precision ~ 2030

Deep inelastic scattering

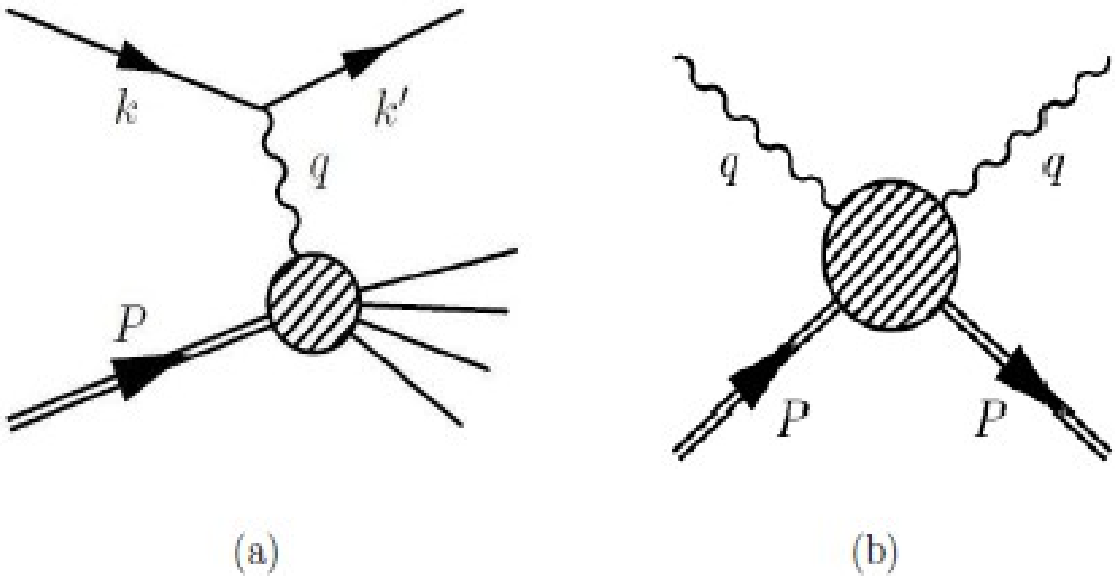

Figure 1: Schematic representation of DIS (a) and FCS (b) processes. k and k' denote the four-momenta of the incoming and outgoing leptons in DIS.

$$\frac{d^2\sigma}{d\Omega\, dE'} = \frac{\alpha_{em}^2}{2Mq^4}\,\frac{E'}{E}\, l_{\mu\nu}\, W^{\mu\nu}$$

DIS cross-section

Bjorken parameter

$$x = -\frac{q^2}{2P\cdot q}$$

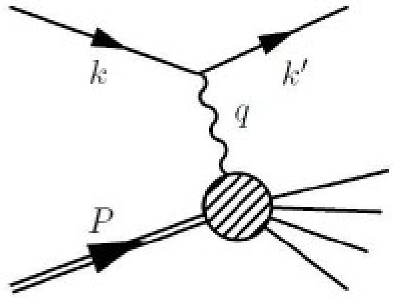

$$W_{\mu\nu} = W^{(\mathrm{S})}_{\mu\nu}(q,P) + i\,W^{(\mathrm{A})}_{\mu\nu}(q,P,S)\,,$$

$$W^{(\mathrm{S})}_{\mu\nu} = \left(\eta_{\mu\nu} - \frac{q_\mu q_\nu}{q^2}\right)\left[F_1(x,q^2) + \frac{1}{2}\frac{S\cdot q}{P\cdot q}g_5(x,q^2)\right],$$
$$-\frac{1}{P\cdot q}\left(P_\mu - \frac{P\cdot q}{q^2}q_\mu\right)\left(P_\nu - \frac{P\cdot q}{q^2}q_\nu\right)\left[F_2(x,q^2) + \frac{S\cdot q}{P\cdot q}g_4(x,q^2)\right]$$
$$-\frac{1}{2P\cdot q}\left[\left(P_\mu - \frac{P\cdot q}{q^2}q_\mu\right)\left(S_\nu - \frac{S\cdot q}{P\cdot q}P_\nu\right) + \left(P_\nu - \frac{P\cdot q}{q^2}q_\nu\right)\left(S_\mu - \frac{S\cdot q}{P\cdot q}P_\mu\right)\right]$$
$$g_3(x,q^2)\,,$$

$$W^{(\mathrm{A})}_{\mu\nu} = -\frac{\varepsilon_{\mu\nu\rho\sigma}q^\rho}{P\cdot q}\left\{S^\sigma g_1(x,q^2) + \left[S^\sigma - \frac{S\cdot q}{P\cdot q}P^\sigma\right]g_2(x,q^2)\right\} - \frac{\varepsilon_{\mu\nu\rho\sigma}q^\rho P^\sigma}{2P\cdot q}F_3(x,q^2)$$

Perturbative QCD

Using DGLAP approximation F_2 can be written as a convolution of coefficient functions which can be calculated to a given order *n* in pQCD for each parton type *i* and nonperturbative but universal PDFs

$$F_2^p(x, Q^2) = \sum_i \int_x^1 \frac{dy}{y} C_i^{(n)}\left(\frac{x}{y}, Q^2\right) f_i^{(n)}(y, Q^2).$$

The PDFs cannot be obtaind from first principles in pQCD, but their virtuality dependence is driven by the DGLAP equations, where their kernels are calculated from pQCD:

$$\frac{df_i^{(n)}(x, Q^2)}{d \log Q^2} = \frac{\alpha_s(Q^2)}{2\pi} \sum_j \int_x^1 \frac{dy}{y} P_{ij}^{(n)}\left(\frac{x}{y}\right) f_j^{(n)}(y, Q^2)$$

BPST Pomeron

We will later discuss on the derivation of the BPST-Pomeron equation for F_2 *(BPST=Brower-Polchinski-Strassler-Tan, 2006)*

$$F_2^{\mathrm{BPST_{HW}}}(x,Q^2) = \frac{g_0^2 \rho^{3/2} Q}{32\pi^{5/2}\tau_b^{1/2} Q'} e^{(1-\rho)\tau_b} \left(e^{-\frac{\log^2(Q/Q')}{\rho\tau_b}} + \mathcal{F}(x,Q,Q') e^{-\frac{\log^2(QQ'z_0^2)}{\rho\tau_b}} \right).$$

$$\mathcal{F}(x,Q,Q') = 1 - 2(\pi\rho\tau_b)^{1/2} e^{\eta^2(x,Q,Q')} \mathrm{erfc}(\eta(x,Q,Q')),$$

$$\eta(x,Q,Q') = \frac{\log(Q'Qz_0^2) + \rho\tau_b}{\sqrt{\rho\tau_b}}, \qquad \tau_b(x,Q,Q') = \log\left(\frac{\rho Q}{2Q'x}\right),$$

g_0^2, ρ, z_0 and Q'.

g_0^2: An overall constant from the particle wavefunctions

ρ: $\rho = 2/\lambda_{\mathrm{t'\,Hooft}}^{1/2}$

z_0: QCD IR cutoff

Q': Order of the proton rest mass

Statistics Minimum

Given a set of parameters $\alpha = \{\alpha_1, ..., \alpha_M\}$ on which depends the function to fit, and

a set of experimental data $y = \{y_1, ..., y_N\}$ measured at the points $x = \{x_1, ..., x_N\}$

E.g. $y_i = F_2(x_i, Q^2)$

$$\Delta\chi_i^2(x_i, \alpha) = \left(\frac{y_i - y(x_i, \alpha)}{\sigma_i}\right)^2 \longrightarrow \chi^2_{\text{total}} = \sum_{i=1}^{N_p} \Delta\chi_i^2$$

$$\chi^2_{\text{d.o.f.}} = \frac{\chi^2_{\text{total}}}{N_{\text{d.o.f.}}}$$

$$P(\chi^2_{\text{total}}, N_{\text{d.o.f.}}) = \frac{1}{2^{N_{\text{d.o.f.}}/2}\,\Gamma[N_{\text{d.o.f.}}/2]} \int_{\chi^2_{\text{total}}}^{\infty} t^{\frac{N_{\text{d.o.f.}}}{2}-1}\, e^{-t/2}\, dt$$

Jorrin, Schvellinger, PRD 2022 & Borsa, Jorrin, Sassot, Schvellinger, 2023

BPST-Pomeron for F_2

Only 4 parameters to fit 280 exp. data

$\rho = 0.7729 \pm 0.0014$, $g_0^2 = 103.73 \pm 0.757$,

$z_0 = 4.894 \pm 0.061\,\text{GeV}^{-1}$, $Q' = 0.4715 \pm 0.0093\,\text{GeV}$.

$\chi^2_{\text{d.o.f.}}$ of 1.086

$P = 0.1535$

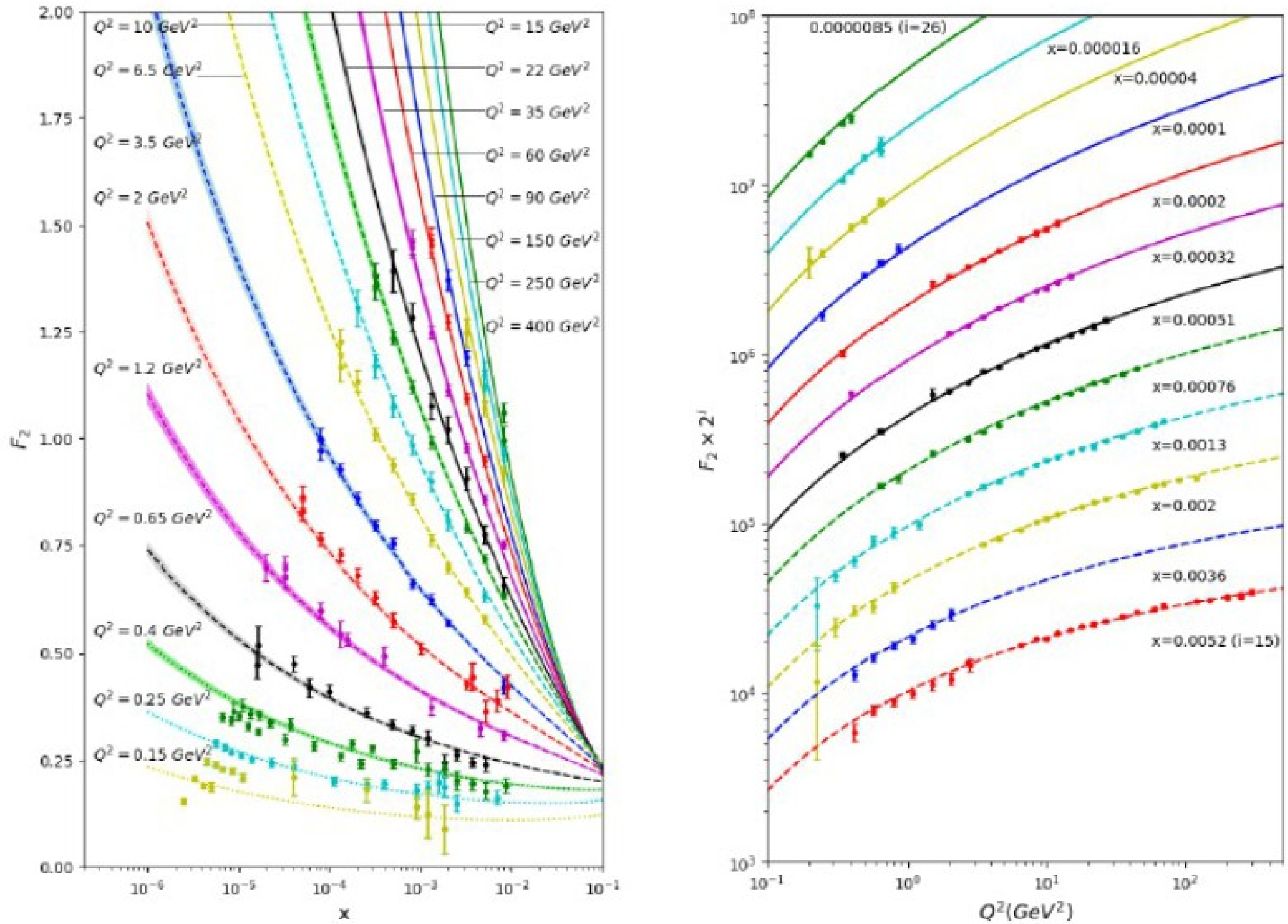

The proton F_2^p structure function using a single BPST Pomeron exchange against data from H1-ZEUS, BCDMS, NMC, E665 and SLAC collaborations within the ranges $0.1\ \text{GeV}^2 < Q^2 \leq 400\ \text{GeV}^2$ and $2.43 \times 10^{-6} \leq x < 0.01$. The number of data points depicted has been limited for a better visualization. Error bands are included in both figures. Due to the logarithmic vertical scale in the right hand side plot, though the error bands are present, they are very narrow and cannot be distinguished from their central values.

Jorrin, Schvellinger, PRD 2022 & Borsa, Jorrin, Sassot, Schvellinger, 2023

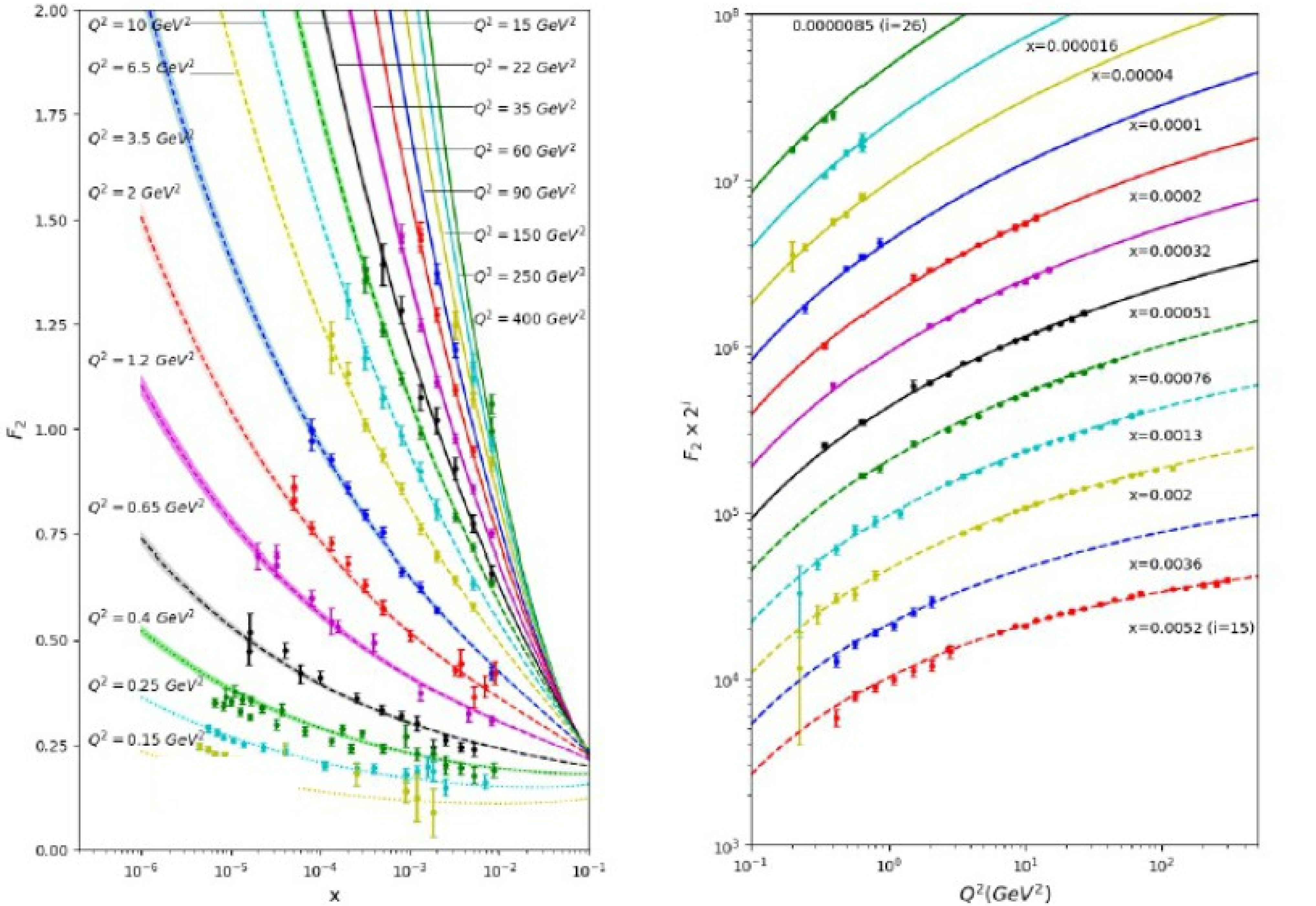

From these parameters

$$\rho = 0.7729 \pm 0.0014, \qquad g_0^2 = 103.73 \pm 0.757,$$
$$z_0 = 4.894 \pm 0.061 \ \mathrm{GeV}^{-1}, \quad Q' = 0.4715 \pm 0.0093 \ \mathrm{GeV}$$

This one: $\rho = 0.7729 \pm 0.0014,$ using: $\rho = 2/\lambda_{\mathrm{t' Hooft}}^{1/2}$

For $N_c=3$ leads to:

$\alpha_{\mathrm{strong}}(Q^2)$ = 0.1776

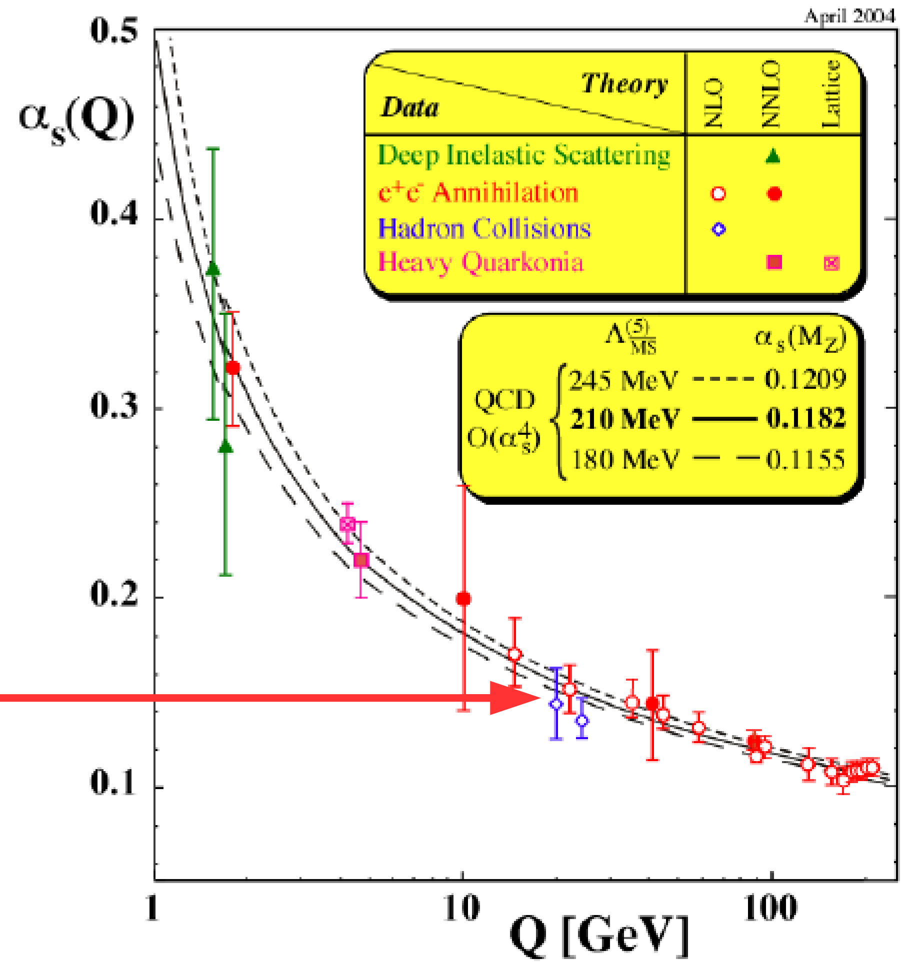

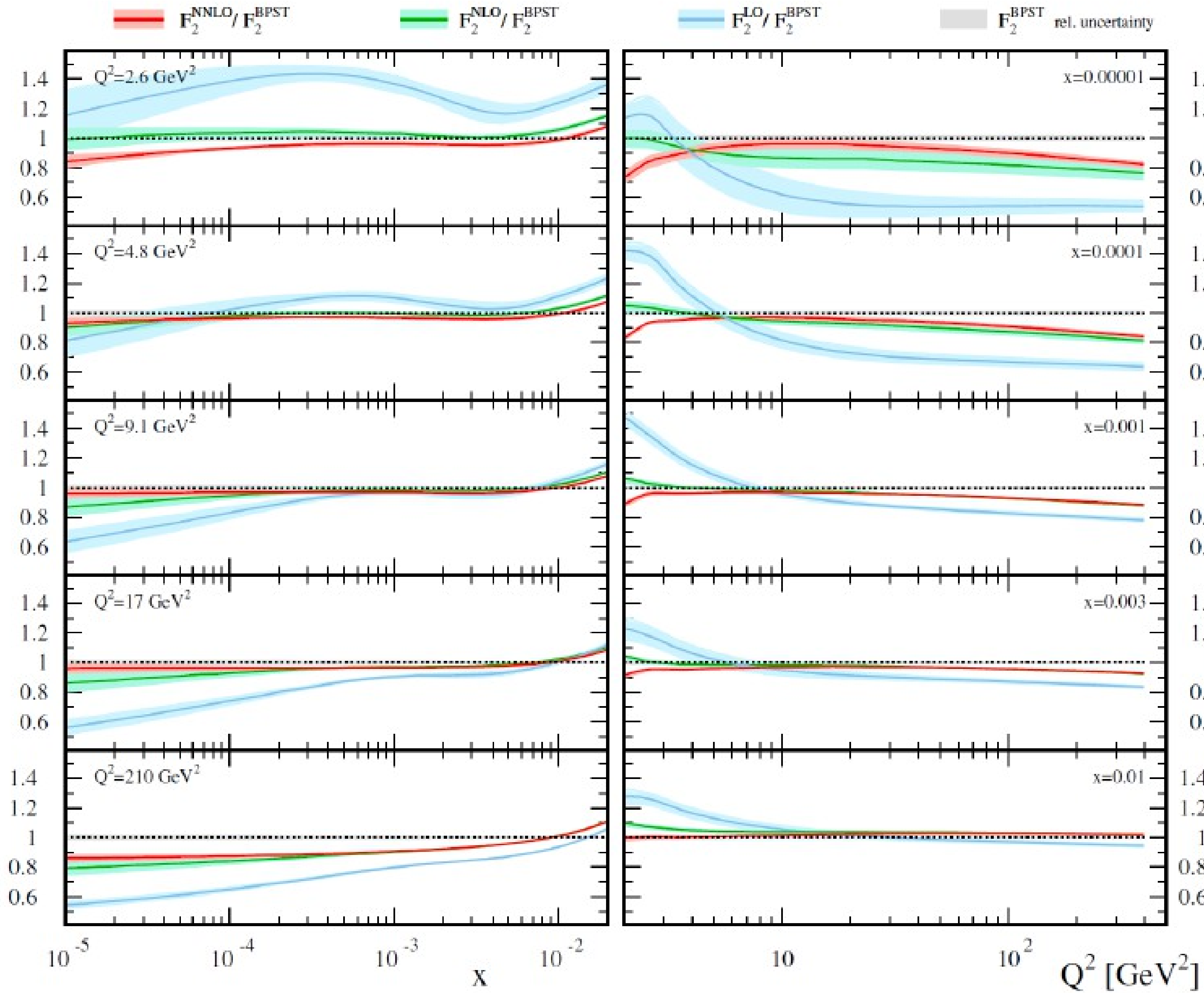

F2NNLO/ F2BPST
F2NLO/ F2BPST
F2LO/ F2BPST
F2BPST rel. uncertainty
Q2=2.6 GeV2
Q2=4.8 GeV2
Q2=9.1 GeV2
Q2=17 GeV2
Q2=210 GeV2
x=0.00001
x=0.0001
x=0.001
x=0.003
x=0.01
1.4
1.2
1
0.8
0.6
10-5
10-4
10-3
10-2
x
10
102
Q2 [GeV2]

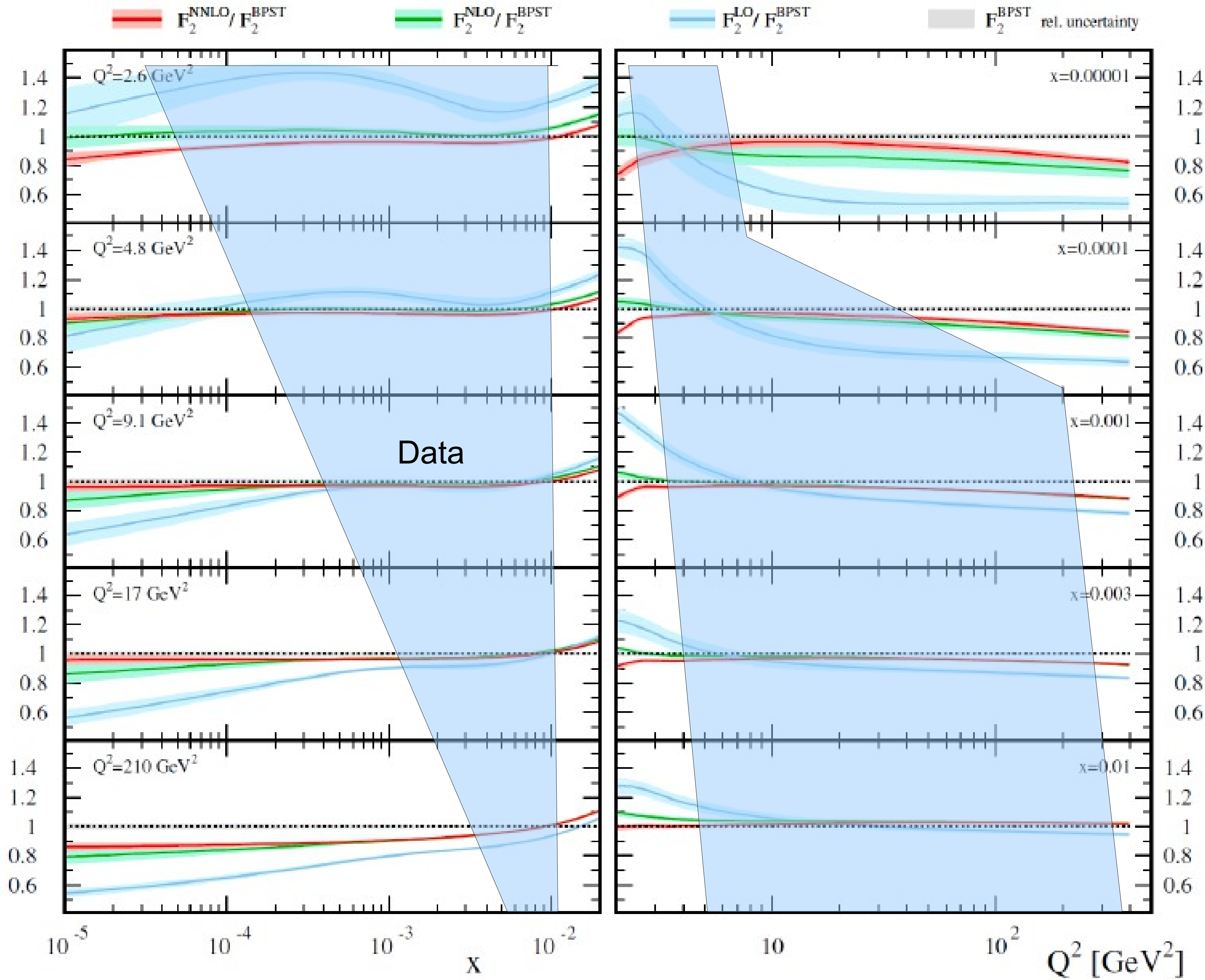

F_2^{NNLO}/F_2^{BPST}
F_2^{NLO}/F_2^{BPST}
F_2^{LO}/F_2^{BPST}
F_2^{BPST} rel. uncertainty
Q^2=2.6 GeV^2
Q^2=4.8 GeV^2
Q^2=9.1 GeV^2
Q^2=17 GeV^2
Q^2=210 GeV^2
x=0.00001
x=0.0001
x=0.001
x=0.003
x=0.01
Data
x
Q^2 [GeV^2]

Electron
Ion
Collider

Polarized electron beam & polarized proton/ion beams

Largest precision ever for polarized DIS

goal: polarized structure function, spin content of proton

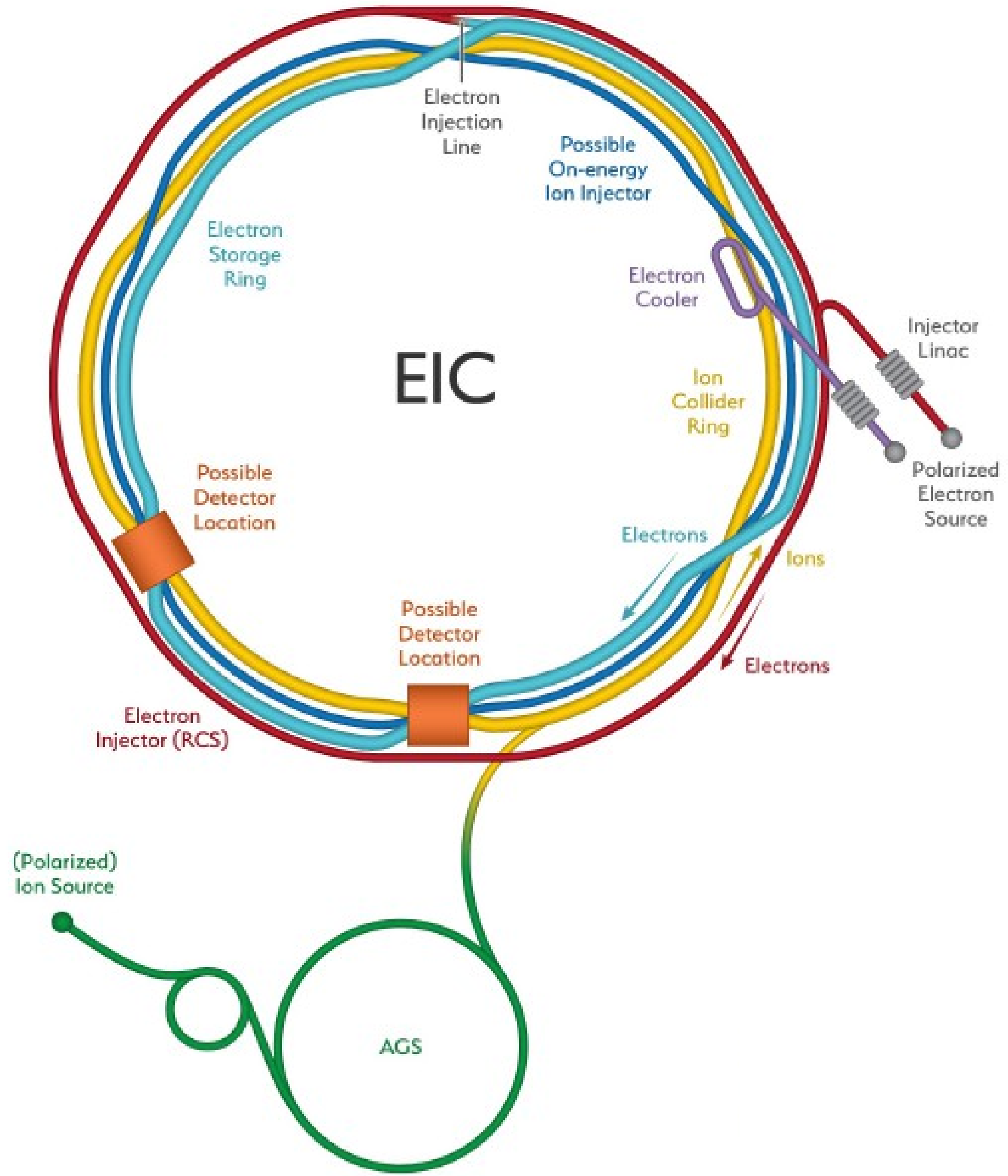

Perturbative QCD for polarized proton

In DGLAP approximation g_1 is written as a convolution of coefficient functions which can be calculated to a given order *n* in pQCD for each parton type *i* and nonperturbative but universal PDFs

$$g_1^p(x,Q^2) = \sum_i \int_x^1 \frac{dy}{y} \Delta C_i^{(n)}\left(\frac{x}{y}, Q^2\right) \Delta f_i^{(n)}(y,Q^2)$$

$$\Delta f_i(x,Q^2) \equiv f_i^{\uparrow}(x,Q^2) - f_i^{\downarrow}(x,Q^2),$$

$$\frac{d\Delta f_i^{(n)}(x,Q^2)}{d\log Q^2} = \frac{\alpha_{\text{strong}}(Q^2)}{2\pi} \sum_j \int_x^1 \frac{dy}{y} \Delta P_{ij}^{(n)}\left(\frac{x}{y}\right) \Delta f_j^{(n)}(y,Q^2).$$

Holographic-A Pomeron

We will later discuss on the derivation of the Holographic-A Pomeron equati[illegible]

$$g_1^{\mathrm{A_4Pomeron_{HW}}}(x, Q^2) = \frac{C\rho^{-1/2} e^{(1-\frac{\rho}{4})\tau_b}}{\tau_b^{1/2}} \left(e^{-\frac{\log^2(Q/Q')}{\rho\tau_b}} + \mathcal{F}(x, Q, Q') e^{-\frac{\log^2(QQ'z_0^2)}{\rho\tau_b}} \right).$$

$$\mathcal{F}(x, Q, Q') = 1 - 2(\pi\rho\tau_b)^{1/2} e^{\eta^2(x,Q,Q')} \mathrm{erfc}(\eta(x, Q, Q')),$$

$$\eta(x, Q, Q') = \frac{\log(Q'Qz_0^2) + \rho\tau_b}{\sqrt{\rho\tau_b}}, \qquad \tau_b(x, Q, Q') = \log\left(\frac{\rho Q}{2Q'x}\right),$$

g_0^2, ρ, z_0 and Q'. Already fixed from F_2

Thus, there is only one free parameter to fix with data from g_1

$$C = 0.145 \pm 0.0015.$$

Experimental data from COMPASS 2015-2017 at SPS-CERN (Super Proton Synchrotron)

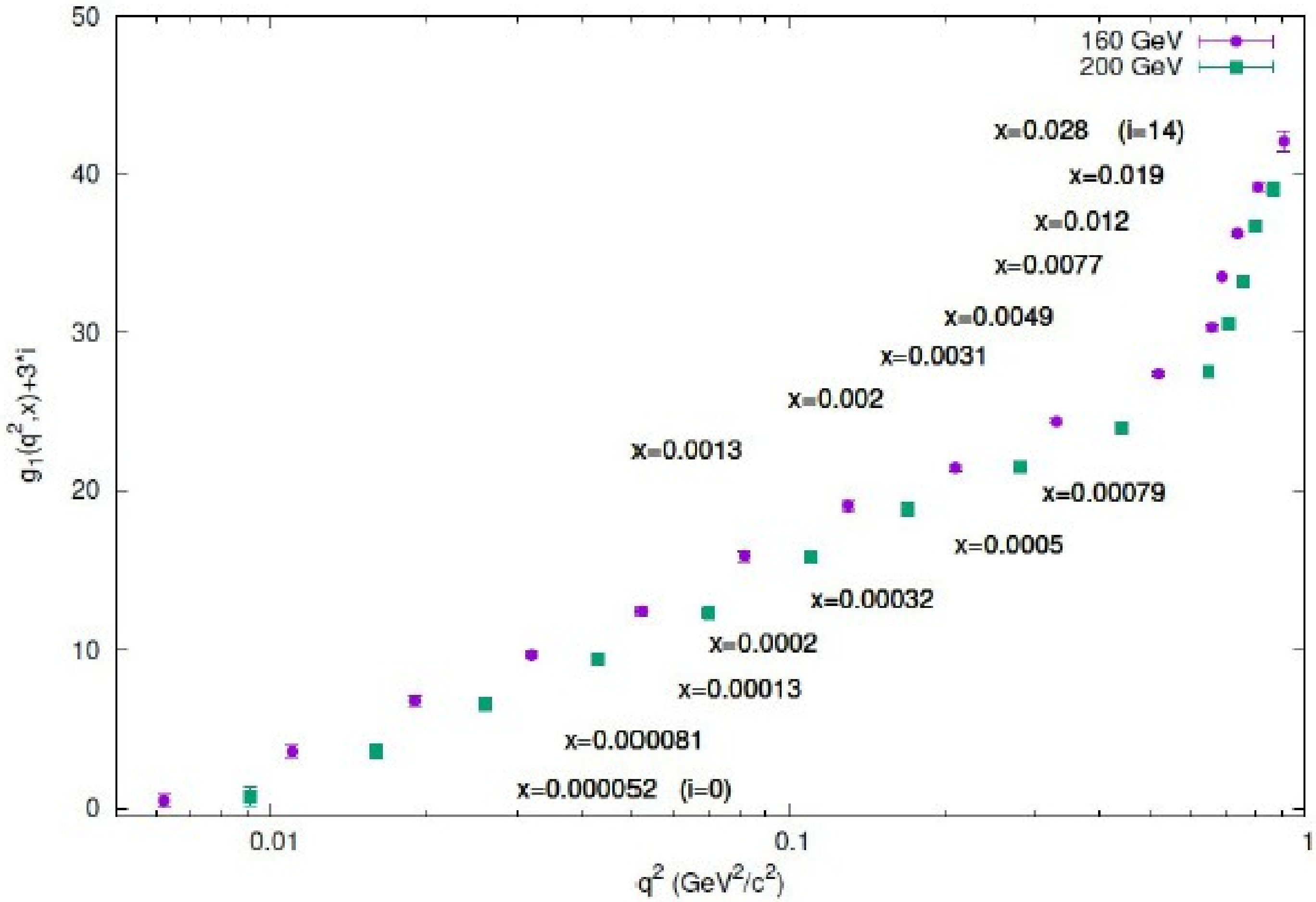

Fitting data, only one parameter, chi^2 per degree of freedom = 1.074, only 30 experimental data

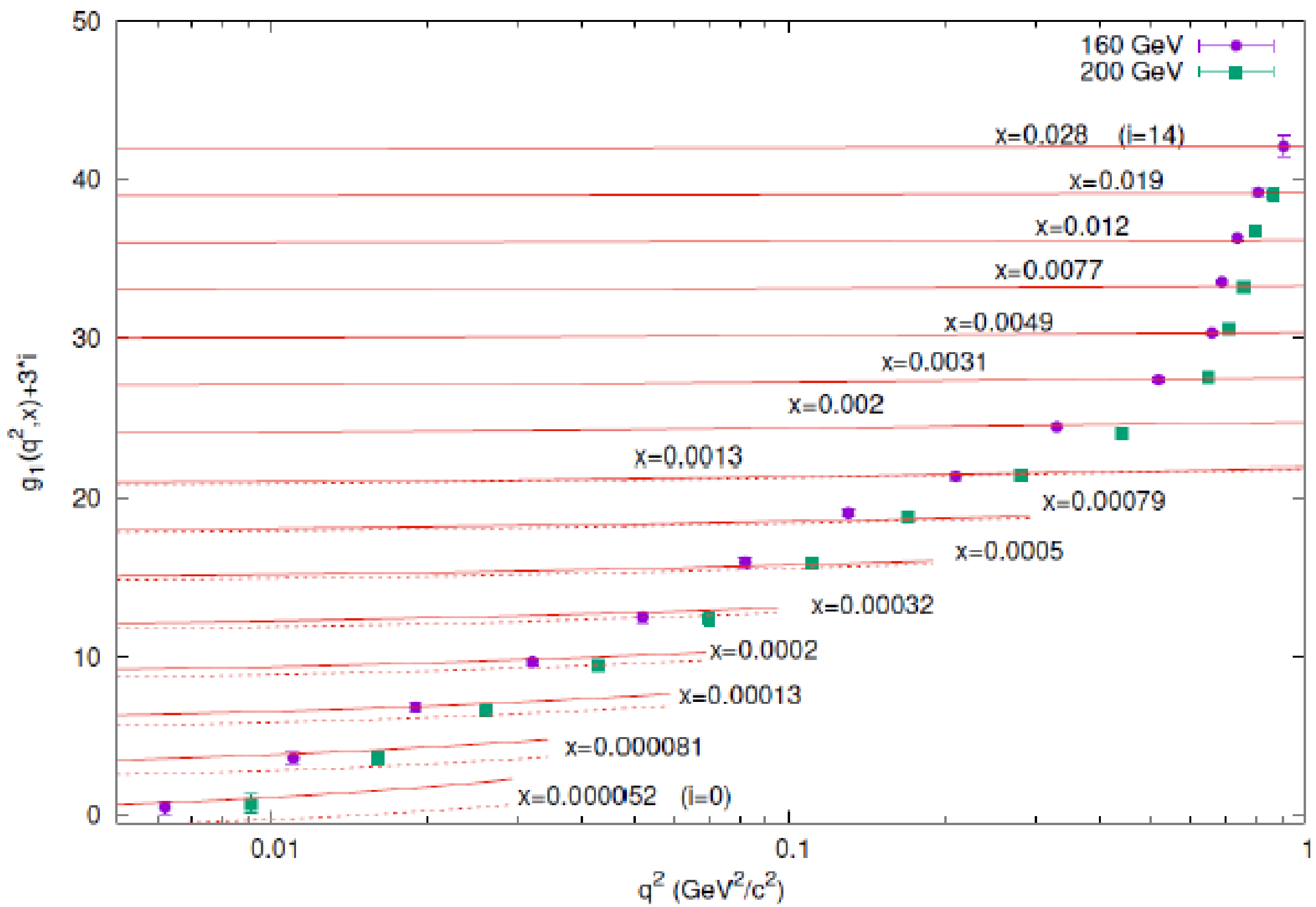

Kovensky, Michalski, Schvellinger, arXiv:1807.11540 [hep-th]

Holographic-A4-Pomeron for g1

$\rho = 0.7729 \pm 0.0014,$ $g_0^2 = 103.73 \pm 0.757,$
$z_0 = 4.894 \pm 0.061\,\text{GeV}^{-1},$ $Q' = 0.4715 \pm 0.0093\,\text{GeV}.$

Only 1 parameter to fit 56 experimental data, C=0.145 +/- 0.0015

$\chi^2_{\text{d.o.f}}$ is 0.94

$P = 0.59$

Jorrin, Schvellinger, PRD 2022

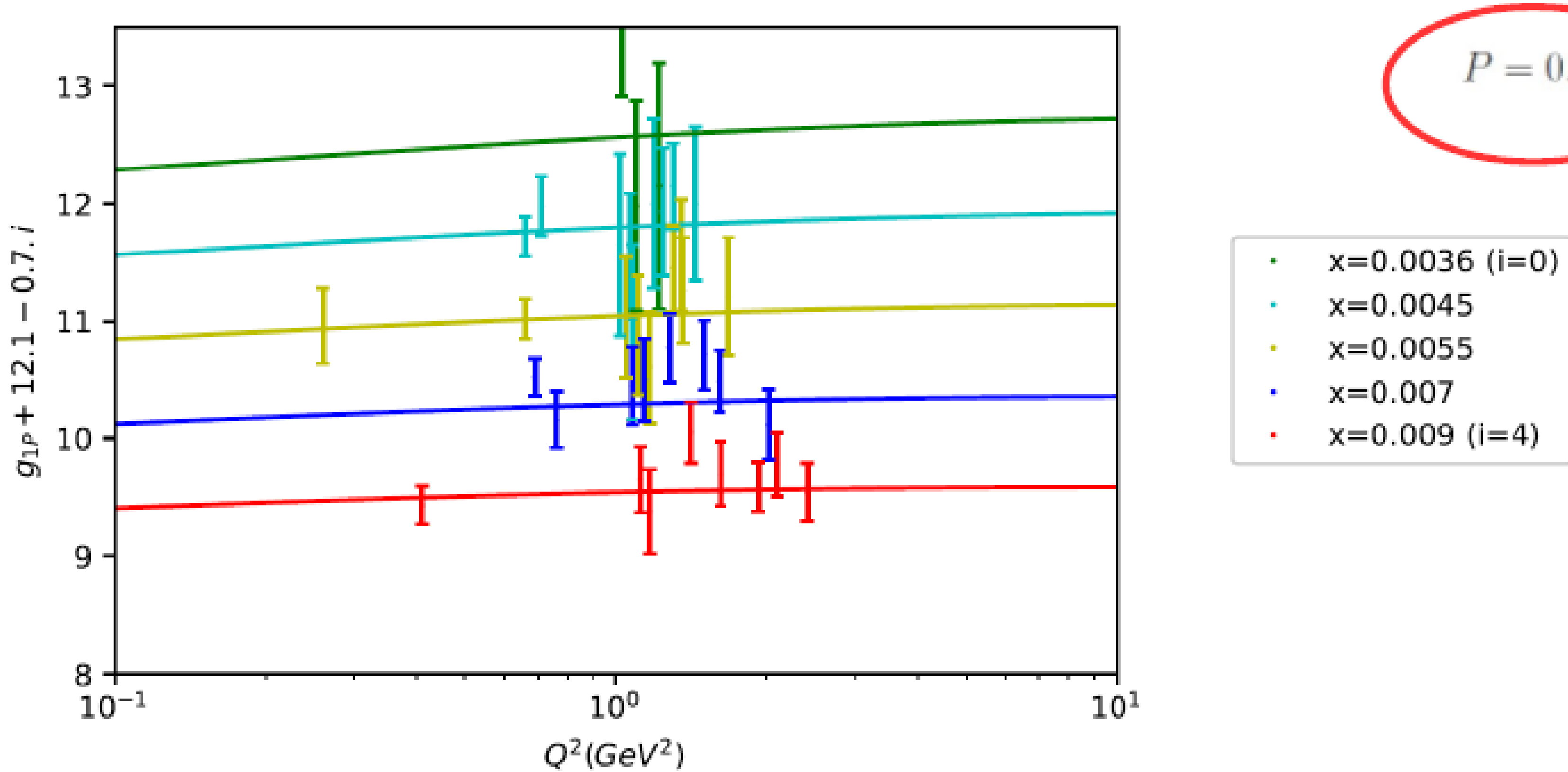

Best fit of the antisymmetric structure function $g_1^{\text{BPST}_{\text{HW}}}(x, Q^2)$ from expression (2.54) in the ranges $0 < x < 0.01$ and $0.1\ \text{GeV}^2 < Q^2 < 400\ \text{GeV}^2$ to data from SMC [61], E143 [62], COMPASS [24, 25, 26] and HERMES [63] collaborations. The parameters ρ, z_0 and Q' have been obtained from the $F_2^{\text{BPST}_{\text{HW}}}(x, Q^2)$ fit. Thus, there is only one free parameter C to fit to a set of 56 points in total from these collaborations. Notice that for each value of x we add a constant $C_i = 12.1 - 0.7i$ to the g_1^P, which goes from 0 ($x = 0.0036$) to 4 ($x = 0.009$).

Holographic-A4-Pomeron for g1

Only 1 parameter to fit experimental data. Kovensky, Michalski, Schvellinger, JHEP 2018

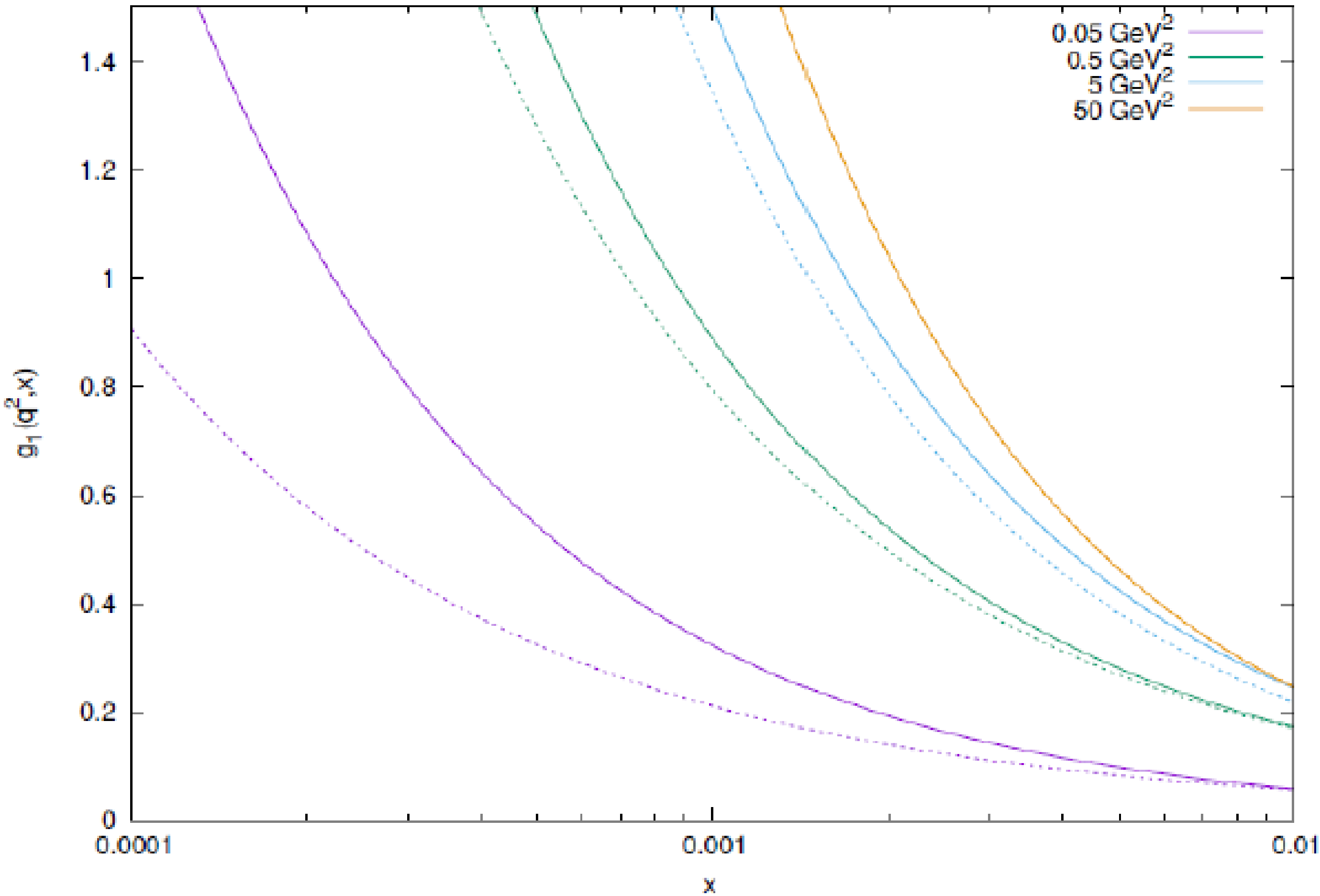

Our results for the structure function g_1. Solid lines correspond to the conformal model. Dotted lines correspond to the hard-wall model. The values of the photon virtuality q^2 are indicated.

Our predictions for the Electron Ion Collider for 2030: using the Holographic-A4-Pomeron for g1

Using only 1 parameter to fit 56 present experimental data

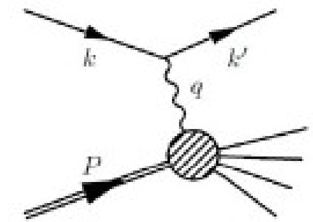

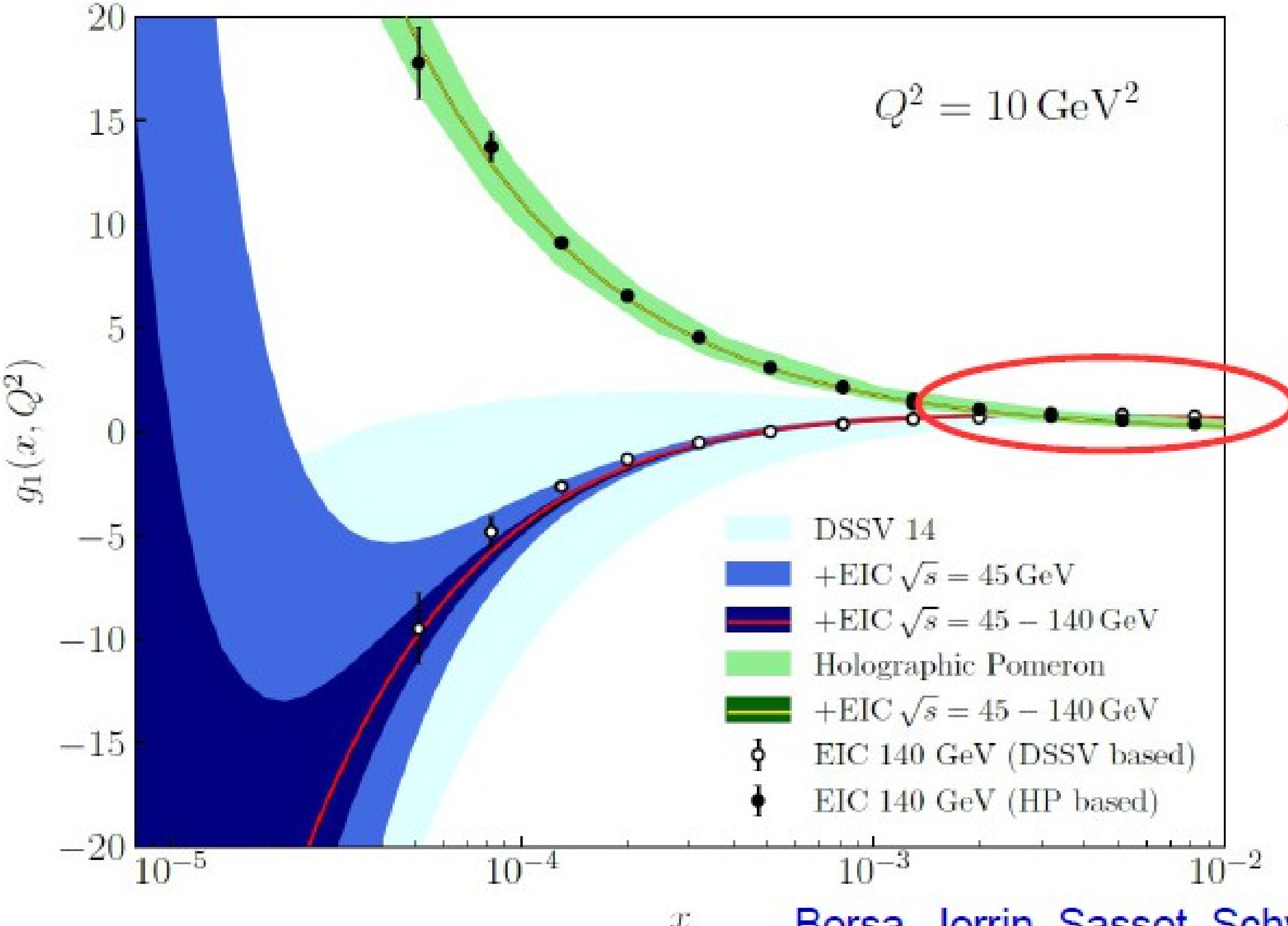

Borsa, Jorrin, Sassot, Schvellinger, 2023

g_1 structure function using a single Holographic-A Pomeron exchange to fit experimental data within the range $0.0036 \leq x \leq 0.009$ at $Q^2 = 10$ GeV^2 against the one obtained in DSSV14 DGLAP NLO analysis.

Global analysis of polarized DIS & SIDIS data with improved small-x helicity evolution

Daniel Adamiak,[1,2] Nicholas Baldonado,[3] Yuri V. Kovchegov,[1] W. Melnitchouk,[2] Daniel Pitonyak,[4]
Nobuo Sato,[2] Matthew D. Sievert,[3] Andrey Tarasov,[5,6] and Yossathorn Tawabutr[7,8]

Spread from BFKL Pomeron

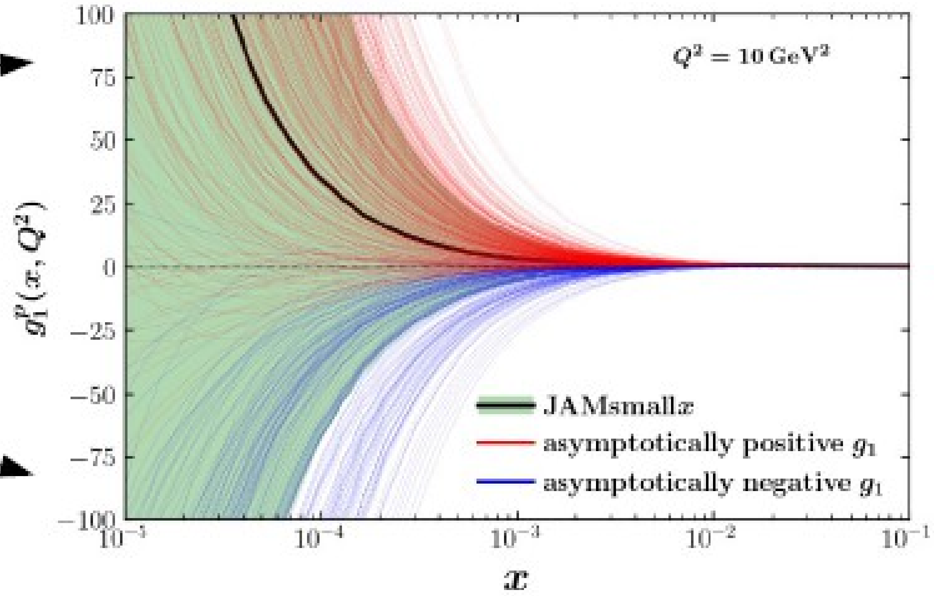

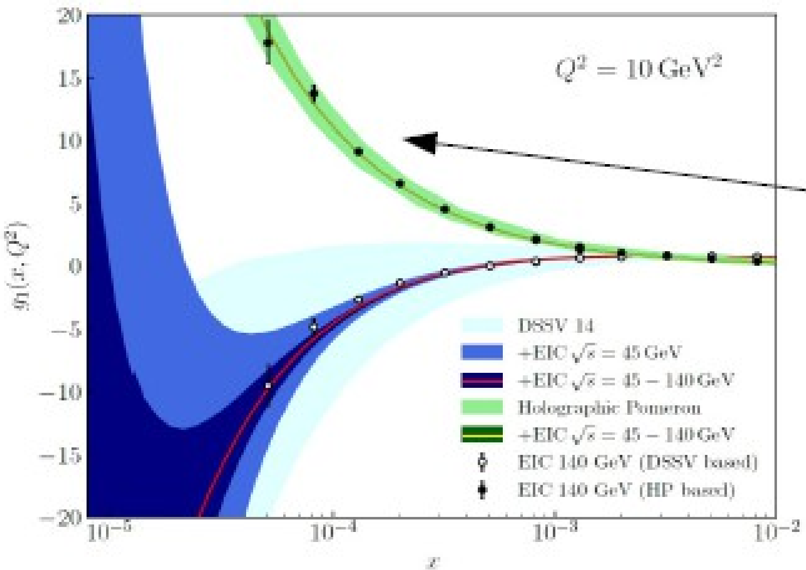

Our Holographic A4 Pomeron

The BPST and Holographic-A Pomerons

Introduction to the AdS/CFT correspondence: The superstring theory side

Consider IIB superstring theory, a D3-brane in Minkowski 10d = 0 1 2 3 4 5 6 7 8 9

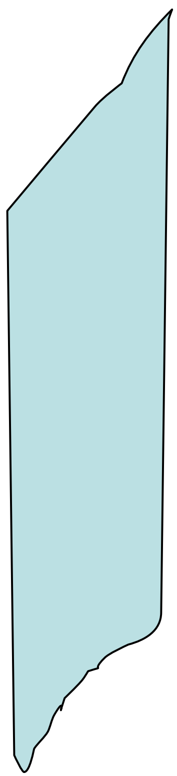

0 1 2 3

A D3-brane picture

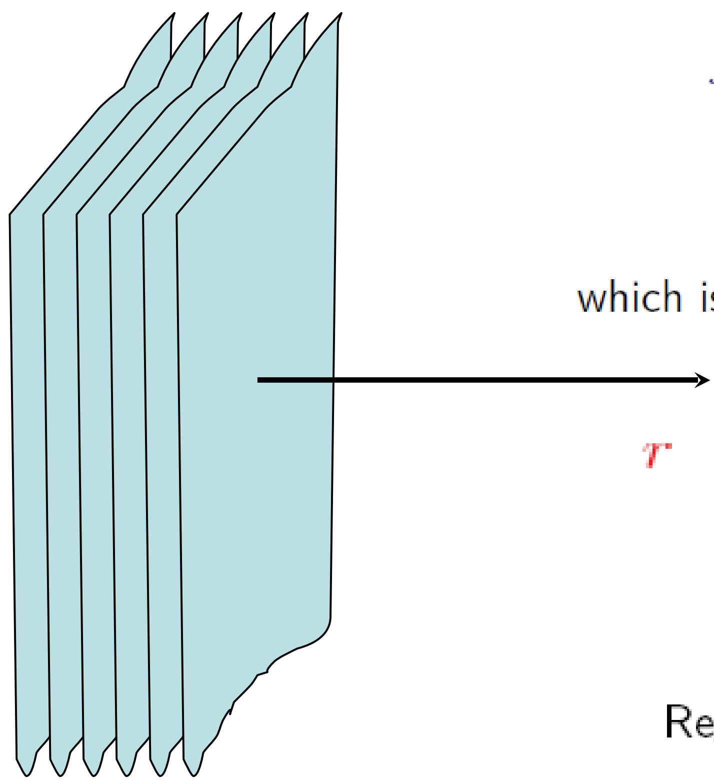

For N coincident D3 branes the induced background metric is

$$\begin{aligned} ds^2 &= f^{-1/2}(r)d\vec{x}^2 + f^{1/2}(r)(dr^2 + r^2 d\Omega_5^2) \\ f(r) &= \left(1 + \frac{L^4}{r^4}\right) \\ L^4 &= 4\pi g_s N(\alpha')^2 \qquad \alpha' = l_s^2 \end{aligned}$$

which is a solution of type IIB supergravity.

Regimes

- $r >> L \rightarrow$ 10d Minkowski
- $r < L \rightarrow$ 10d throat
- $r << L \rightarrow AdS_5 \times S^5$

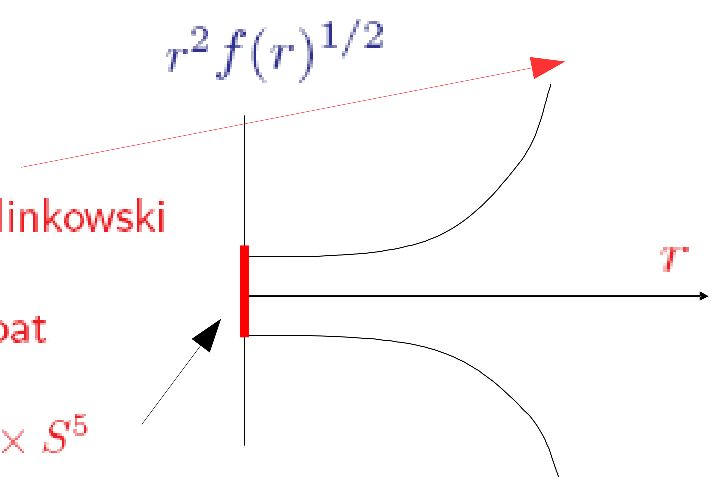

After changing variables $r \longrightarrow z = \frac{L^2}{r}$ and taking the decoupling limit

$$\lim_{\alpha' \to 0,\ r \to 0} z = \lim_{\alpha' \to 0,\ r \to 0} \frac{L^2}{r} = const$$

the metric becomes $AdS_5 \times S^5$

$$ds^2 \quad = \quad \frac{L^2}{z^2}(d\vec{x}^2 + dz^2 + z^2 d\Omega_5^2)$$

AdS_5 has a boundary which is 4d Minkowski spacetime.

Gauge/strings duality minimum

From type IIB superstring theory, we have a solution which is the near horizon limit a stack of *N* D3-branes:

$$\mathrm{AdS}_5 \times S^5$$

$$ds^2 = \frac{r^2}{R^2}\eta_{\mu\nu}dx^\mu dx^\nu + \frac{R^2}{r^2}dr^2 + R^2 d\Omega_5^2, \qquad R = (4\pi\lambda_{\text{'t Hooft}}\alpha'^2)^{1/4}$$

with constant dilaton and *N* units of the flux of F_5 on the 5 sphere. The rest of the fields are set to zero.

We need to introduce a confinement scale → $\Lambda \equiv r_0/R^2$

This is of the order of the glueball mass

The conserved four-momentum in the dual gauge theory is $p^\mu_{4d} = -i\partial/\partial x_\mu$

This is related to the 10-momentum through: $p^\mu_{4d} = \frac{r}{R}\tilde{P}^\mu_{10d}$.

This implies that a string theory scattering process localized at position r in $\mathrm{AdS}_5 \times S^5$ corresponds to a particle scattering with four-momentum p^μ_{4d}

IR deformed $\mathcal{N} = 4$ SYM theory $\qquad \lambda_{\text{'t Hooft}} \equiv g^2_{\text{YM}} N_c$

BPST and Holographic-A Pomerons

The 10D space where the closed string propagates can be written as

$$X^M(\sigma_1, \sigma_2) = x^M + X'^M(\sigma_1, \sigma_2)$$

Taking the Gaussian integral over X' s, the 10D S-matrix as seen by a local observer is

$$S = i \int d^4x \int d^6y \sqrt{-G} A_{\rm local}(x, y)$$

This is a local approximation that can be written in terms of the flat 10D amplitude

$$A_{\rm local}(x, y) \to \tau_{10}(\tilde{P}) \prod_{i=1}^{4} e^{ip_i \cdot x_i} \Psi(y_i)$$

BPST and Holographic-A Pomerons

Then

$$S = i(2\pi)^4\delta^{(4)}\left(\sum_{i=1}^{4} p_i\right)\int d^6y\sqrt{-G_{6d}}\,\tau_{10}(\tilde{P})\prod_{i=1}^{4}\Psi(y_i)$$

From the metric warp factor we have an IR red-shift!!!

$$\tilde{P}^{\mu}_{10\mathrm{d}} = \frac{R}{r}p^{\mu}_{4\mathrm{d}} \longrightarrow \tilde{s}_{10\mathrm{d}} = \frac{R^2}{r^2}s \quad \text{and} \quad \tilde{t}_{10\mathrm{d}} = \frac{R^2}{r^2}t.$$

On the other hand, from superstring theory:

$$\tau_{10}(\tilde{P}) = g^2_{\mathrm{string}}\alpha'^3 F_s(\tilde{P}\sqrt{\alpha'}),$$

$$\downarrow$$

$$F_s(\tilde{P}\sqrt{\alpha'}) = K(\tilde{P}\sqrt{\alpha'})\left[\prod_{\tilde{x}=\tilde{s},\tilde{t},\tilde{u}}\frac{\Gamma(-\alpha'\tilde{x}/4)}{\Gamma(1+\alpha'\tilde{x}/4)}\right]$$

BPST and Holographic-A Pomerons

Then, for $|\tilde{t}| \ll \tilde{s}$, $$F_s\left(\tilde{P}\sqrt{\alpha'}\right) \approx K(\tilde{P}\sqrt{\alpha'})\frac{\Gamma(-\alpha'\tilde{t}/4)}{\Gamma(1+\alpha'\tilde{t}))}(\alpha'\tilde{s})^{2+\alpha'\tilde{t}/2}$$
$$= f(\alpha'\tilde{t})(\alpha'\tilde{s})^{2+\alpha'\tilde{t}/2},$$

The 4D amplitude becomes

$$\tau_4(s,t)$$
$$= \int d^6y\sqrt{-G}\Psi_3(y)\Psi_4(y)f(\alpha'\tilde{t})(\alpha'\tilde{s})^{2+\alpha'\tilde{t}/2}\Psi_1(y)\Psi_2(y).$$

Thus, the relevant exponent is $j = 2 + \alpha'\tilde{t}/2 = 2 + \alpha' tR^2/(2r^2)$

The maximum contribution for t>0 is

$$j_{\text{Max}} = 2 + \alpha'\tilde{t}/2 = 2 + \alpha' tR^2/(2r_0^2)$$

This leads to the Regge behavior for t>0

BPST and Holographic-A Pomerons

when $t < 0$ the maximum value of the exponent is:

$$j_{\mathrm{Max}} = 2$$

this is the UV region of the gauge theory

the hard and sof Pomerons become unified

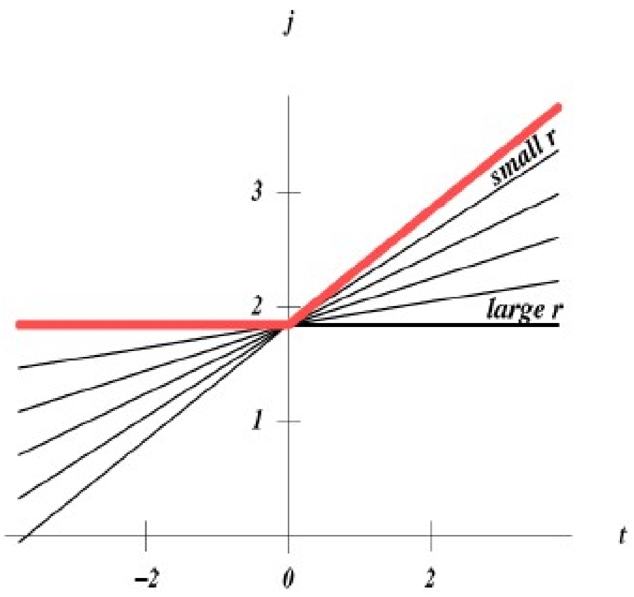

BPST Pomeron

At low *x*: the following diagrams contribute

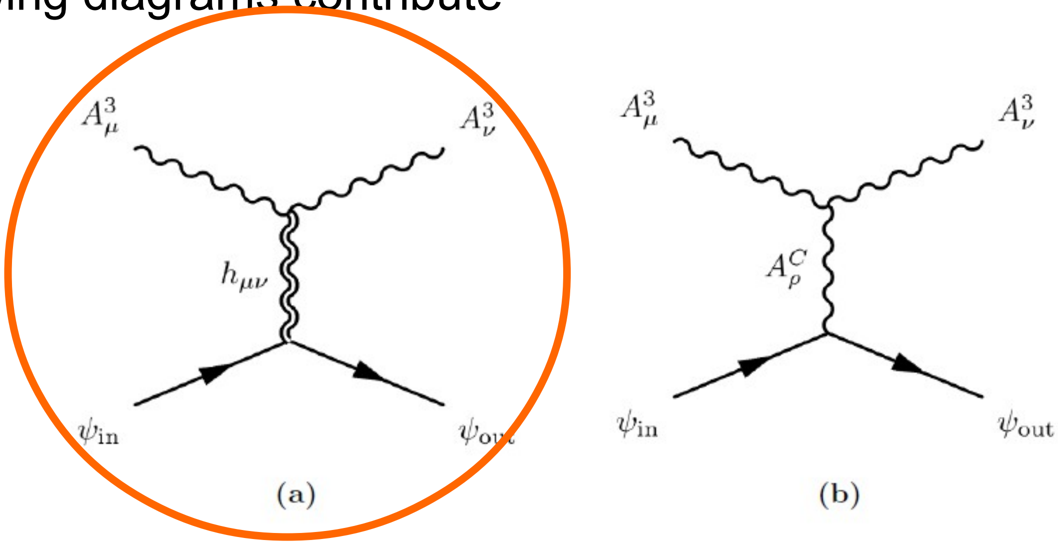

Which come from the effective 5d action on AdS_5 from dimensional reduction of the type IIB superstring low energy action on S^5

$$S_{5d} = \frac{1}{2\kappa_5^2}\int d^5x\sqrt{-g_{AdS_5}}\left(\mathcal{R} - \bar{\psi}\,\gamma^m D_m\psi - \frac{1}{4}\,(F^A_{mn})^2 + \cdots\right)$$

$$\Psi(x^m,\Omega) = \sum_\Delta \psi_\Delta(x^m)\otimes\eta_\Delta(\Omega)\,, \quad h^{ma} = \sum_k A^m_k(x^n)\,Y^a_k(\Omega)$$

This contributes to F2

Holographic-A Pomeron

At low x: the following diagrams contribute

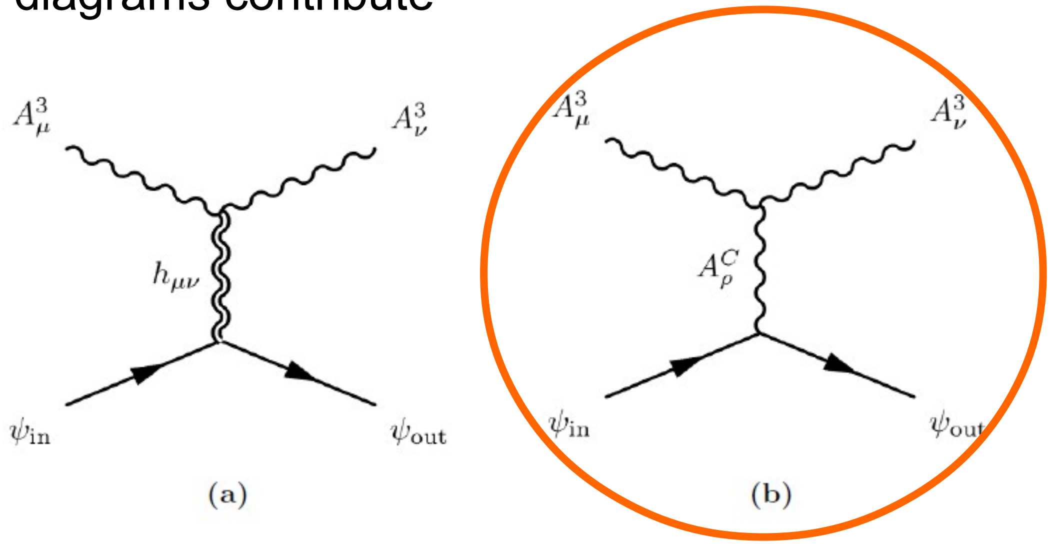

$$A_m^A \equiv B_m^A - \frac{16}{R}\tilde{B}_m^A$$

In addition, from 5 dimensional SU(4) SUGRA on AdS5 there are the Chern-Simons and the Pauli terms:

$$S_{\rm CS} = \frac{i\ \kappa}{96\pi^2} d_{ABC} \int d^5x\, \varepsilon^{mnopq}\, A_m^A\, \partial_n A_o^B\, \partial_p A_q^C \qquad S_P = \beta^A \int d^5x\, \sqrt{-g_{\rm AdS}}\, F_{mn}^A\, \bar{\psi}\, [\gamma^m, \gamma^n]\, \psi$$

$$\Psi(x^m, \Omega) = \sum_\Delta \psi_\Delta(x^m) \otimes \eta_\Delta(\Omega)\,,$$

$$h_{ma} = \sum_k B_m^{(k)}(x^n)\, Y_a^{(k)}(\Omega)\,, \qquad a_{mabc} = \sum_k \tilde{B}_m^{(k)}(x^n)\, \epsilon_{abc}{}^{de}\, \nabla_d Y_e^{(k)}(\Omega)$$

These contribute to g1

BPST and Holographic-A Pomerons

The corrections to that exponent $j = 2 + \alpha' \tilde{t}/2 = 2 + \alpha' t R^2/(2r^2)$

can be obtained by replacing

$$\alpha' \tilde{t} \to \alpha' \nabla_P^2 \equiv \alpha' \frac{R^2}{r^2} t + \alpha' \nabla_\perp^2$$

$\nabla_\perp^2$ is proportional to $\alpha' / R^2 = \lambda_{\text{'t Hooft}}^{-1/2}$

In the light cone this operator acting on a fluctuation of a bulk field becomes

$$\nabla_2^2 \Phi_{++} = \frac{r^2}{R^2} \nabla_0^2 \left(\left(\frac{R^2}{r^2} \right) \Phi_{++} \right) + \frac{1}{2} \mathcal{R}_+^+$$

$$j_0 = 2 - \frac{2}{\lambda_{\text{t' Hooft}}^{1/2}}$$

$$\mathrm{Im}_{\mathrm{exc}}\left[G(\alpha', \tilde{s}, \tilde{t}, \tilde{u})\ \tilde{s}^2\right]|_{\tilde{t}\to 0} = \frac{\pi\alpha'}{4}\sum_{m=1}^{\infty}\delta\left(m - \frac{\alpha'\tilde{s}}{4}\right)(m)^{\alpha'\tilde{t}/2}$$

Consistent treatment of The 10D t-channel

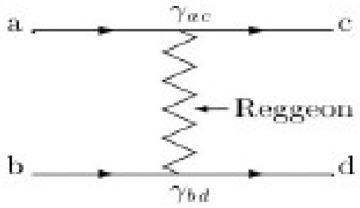

$$\mathcal{A} = 2s\int d^2b\int dz dz'\, P_A(z)P_\psi(z')\,\chi(z,z',s,b)|_{t=0}$$

$$F_2(x,q^2) \sim \int \frac{dz}{z}\frac{dz'}{z'}P_A(z,q^2)P_\psi(z')(zz'q^2)\,\frac{e^{\zeta(1-\rho)}}{\sqrt{\zeta}}\left(e^{-\frac{\log^2(z/z')}{\rho\zeta}} + \mathcal{F}(z,z',\zeta)e^{-\frac{\log^2\left(zz'/z_0^2\right)}{\rho\zeta}}\right)$$

$$P_A(z,q^2) = (qz)^2\left(K_1^2(qz) + K_0^2(qz)\right)\ ,\ P_\psi(z') = z^{-3}|f_+(z')|^2 \sim (z'\Lambda)^{2\tau-2}$$

$$g_1(x,q^2) \;=\; \frac{\mathcal{Q}\pi^2}{24}\int dy\, dy'\,\mathcal{P}_A(y,q)P_\psi(y')\ \times$$
$$\frac{e^{\zeta(1-\rho/4)}}{\sqrt{\pi\zeta\rho}}\left(e^{-\frac{\sqrt{\lambda}}{8\zeta}(y-y')^2} + \mathcal{F}(y,y',\zeta)e^{-\frac{\sqrt{\lambda}}{8\zeta}(y+y')^2}\right)$$

Kovensky, Michalski & MS, arXiv:1807.11540 [hep-th]

$$y = -2\log(z).$$

$$\mathcal{P}_A(z,q^2) = (qz)^3K_1(qz)K_0(qz)$$

Holographic-A Pomeron

$$\text{Im}_{\text{exc}}\left[\mathcal{G}(\alpha', \tilde{s}, \tilde{t}, \tilde{u})\ \tilde{s}^2\right]|_{\tilde{t}\to 0} = \frac{\pi\alpha'}{4}\sum_{m=1}^{\infty}\delta\left(m - \frac{\alpha'\tilde{s}}{4}\right)(m)^{\frac{\alpha'\tilde{t}}{2}},$$

$$\frac{\alpha'\tilde{t}}{2} = \frac{1}{2}\frac{\alpha'}{R^2}z^2 t + \frac{1}{2}\frac{\alpha'}{R^2}(\Delta_1 + 3) = \frac{1}{2}\frac{\alpha'}{R^2}z^2 t + \frac{1}{2\sqrt{\lambda}}\left[z^2\partial_z^2 - z\partial_z\right]$$

By introducing $\rho = 2u = -2\ln(z/z_{\text{ref}})$ we can rewrite $\Delta_1 + 3 = 4(\partial_\rho^2 + \partial_\rho)$.

$$\mathcal{K}_\Lambda(\rho, \rho', t = 0, j = 1) = (\alpha'\tilde{s})^{1-\frac{1}{2\sqrt{\lambda}}}\, e^{-\frac{1}{2}(\rho+\rho')} \times\sqrt{\frac{\lambda^{1/2}}{2\pi\tau}}\left[e^{-\frac{\sqrt{\lambda}}{8\tau}(\rho-\rho')^2} + F(\rho/2, \rho'/2, \tilde{\tau})e^{-\frac{\sqrt{\lambda}}{8\tau}(\rho+\rho')^2}\right]$$

The Regge slope is now $1 - 1/(2\sqrt{\lambda})$

This contributes to g1 and corresponds to the Reggeization of $A_m^A \equiv B_m^A - \frac{16}{R}\tilde{B}_m^A$

Holographic-A Pomeron

$$\mathrm{Im}_{\mathrm{exc}}\left[\mathcal{G}(\alpha', \tilde{s}, \tilde{t}, \tilde{u})\ \tilde{s}^2\right]|_{\tilde{t}\to 0} = \frac{\pi\alpha'}{4}\sum_{m=1}^{\infty}\delta\left(m - \frac{\alpha'\tilde{s}}{4}\right)(m)^{\frac{\alpha'\tilde{t}}{2}},$$

$$\frac{\alpha'\tilde{t}}{2} = \frac{1}{2}\frac{\alpha'}{R^2}z^2 t + \frac{1}{2}\frac{\alpha'}{R^2}(\Delta_1 + 3) = \frac{1}{2}\frac{\alpha'}{R^2}z^2 t + \frac{1}{2\sqrt{\lambda}}\left[z^2\partial_z^2 - z\partial_z\right]$$

By introducing $\rho = 2u = -2\ln(z/z_{\mathrm{ref}})$ we can rewrite $\Delta_1 + 3 = 4(\partial_\rho^2 + \partial_\rho)$.

$$\mathcal{K}_\Lambda(\rho, \rho', t = 0, j = 1) = (\alpha'\tilde{s})^{1-\frac{1}{2\sqrt{\lambda}}}\, e^{-\frac{1}{2}(\rho+\rho')} \times\sqrt{\frac{\lambda^{1/2}}{2\pi\tau}}\left[e^{-\frac{\sqrt{\lambda}}{8\tau}(\rho-\rho')^2} + F(\rho/2, \rho'/2, \tilde{\tau})e^{-\frac{\sqrt{\lambda}}{8\tau}(\rho+\rho')^2}\right]$$

The Regge slope is now $1 - 1/(2\sqrt{\lambda})$

This contributes to g1 and corresponds to the Reggeization of $A_m^A \equiv B_m^A - \frac{16}{R}\tilde{B}_m^A$

Conclusions

- Excellent fit for F2 and g1 for the proton
- Precise predictions for future spin proton experiments at the EIC